ARTICLE

Effect of Water Vapor Absorption on Measurements of Atmospheric Nitrate Radical by LP-DOAS

Su-wen Li[a*], Wen-qing Liu[b], Pin-hua Xie[b], Yi-jun Yang[a], De-bao Chen[a], Zheng Li[a]

a. Department of Physics, Huaibei Coal Industry Teachers College, Huaibei 235000, China
b. Key Laboratory of Environmental Optical and Technology, Anhui Institute of Optics and Fine Mechanics, Chinese Academy of Sciences, Hefei 230031, China

(Dated: Received on May 6, 2008; Accepted on June 12, 2008)

During the measurement of atmospheric nitrate radical by long-path differential optical absorption spectroscopy, water vapor strong absorption could affect the measurement of nitrate radical and detection limits of system. Under the tropospheric condition, the optical density of water vapor absorption is non-linearly dependent on column density. An effective method was developed to eliminate the effect of water vapor absorption. Reference spectra of water vapor based on the daytime atmospheric absorption spectra, when fitted together with change of cross section with water vapor column densities, gave a more accurate fitting of water vapor absorptions, thus its effect on the measurements of nitrate radical could be restricted to a minimum and detection limits of system reached 3.6 ppt. The modified method was applied during an intensive field campaign in the Pearl River Delta, China. The NO_3 concentration in polluted air masses varied from 3.6 ppt to 82.5 ppt with an average level of 23.6±1.8 ppt.

Key words: Nitrate radical, Water vapor absorption, Long-path differential optical absorption spectroscopy, Detection limit

I. INTRODUCTION

Nocturnal chemistry and physics are important to conserve air quality, which determines initial conditions for photochemistry during the following day. Nitrate radical (NO_3) has been found to act as important initiator of the nighttime degradation of many volatile organic compounds (VOCs) and dimethylsulphide [1-5]. The nitrate radical also plays a key role in the non-photochemical conversion of nitrogen oxides to HNO_3 [6-10].

The in-time and in-line measurement of NO_3 is an instrument challenge because of its extremely low ambient concentration and high spatial and temporal variability. Several measurement techniques have been successfully established: long path differential optical absorption spectroscopy (LP-DOAS) [1,4-6], cavity ring-down spectroscopy (CRDS) [2,7], ion drift chemical ionization mass spectrometry (ID-CIMS) [8], and matrix isolation electron spin resonance (MIESR) [10]. DOAS is used as a standard for the instrument inter-comparison because it is inherently calibrated. DOAS uses the narrow molecular absorption bands to identify trace gases and their absorption strength to retrieve trace gases concentration. The major advantage of DOAS is the ability to measure concentration of trace gases without disturbing their chemical behavior. The other techniques require frequent sophisticated field calibrations or need to sample from ambient air. Therefore, LP-DOAS is developed to measure the NO_3 radical [9-13].

Following its first detection using LP-DOAS in the troposphere by Platt *et al.* [11], the study on oxidation capacity and loss processes of nitrate radical has become one of the international advanced areas of research. With the method of LP-DOAS, we have started to measure nighttime atmospheric nitrate radical in China since December, 2005 [6,12]. Due to its low concentration, water vapor strong absorption in the measuring band could affect evaluation of nitrate radicals, and the absorption of water vapor is non-linearly dependent on column density.

In this work, an effective method was presented. It was possible to account for non-linearity and varying water vapor columns by fitting together with reference spectra of water vapor and change of cross section with water vapor column densities. Finally, the modified method was applied during an intensive field campaign in the Pearl River Delta, China.

II. DOAS MEASUREMENT FOR NO_3

The NO_3 radical was measured along a 3.0 km optical path using LP-DOAS. Figure 1 is the schematic view of a LP-DOAS experimental setup for NO_3. The light source was a 150 W Xenon high pressure lamp. A Cassegrain telescope is used to transmit and receive light, which is reflected by an array of 13 retro-reflectors. Through a 7×0.1 mm diameter fiber bundle, which is regulated by a mode mixer to reduce the interference fringe produced by the total reflec-

*Author to whom correspondence should be addressed. E-mail: suwen_li@yahoo.cn

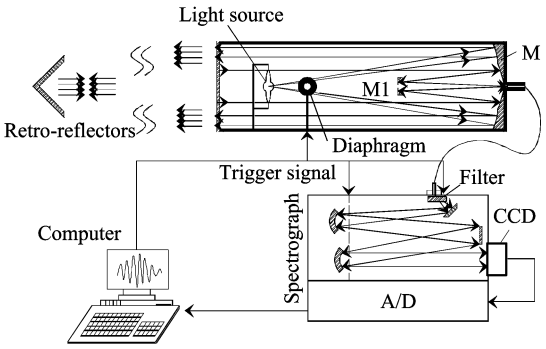

FIG. 1 Schematic view of a LP-DOAS experimental setup for NO_3.

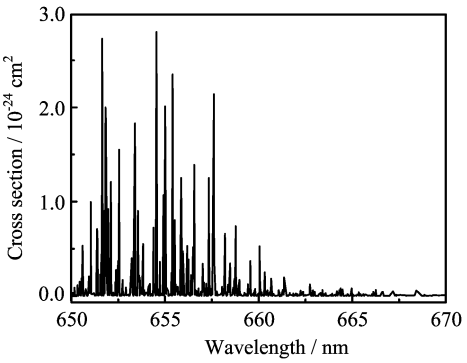

FIG. 2 Calculated absorption lines of water vapor absorption at the high resolution of 5 μm.

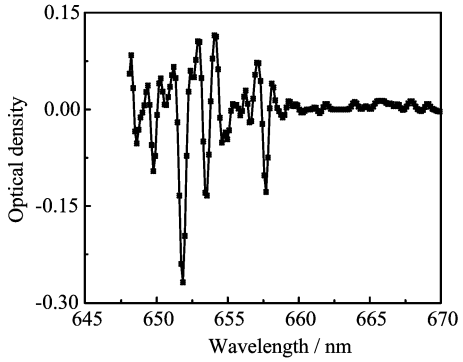

FIG. 3 Calculated optical densities of water vapor absorption at low resolution.

tions inside the fiber of the light leaving the fiber, the light is transmitted to the spectrograph and then to the detector. The spectrograph is an Andor Shamrock SR-303i with focal length of 303 nm, a linear dispersion of 2.6 nm/mm and a diffraction grating with 600 grooves/mm. In order to reduce dark current, the Andor iDUS CCD detector was cooled down to −45 °C by a Peltier cascade. A 610 nm long pass red filter, to reduce stray light effects below 610 nm, is placed in the fiber optic coupler. Finally, the spectral signal is stored and analyzed in the computer. The integration time of the measurement spectra is adjusted automatically to the incoming light intensity [12].

The concentration of NO_3 can be retrieved by applying the Lambert-Beer's law [13-23]:

$$I(\lambda) = I_0(\lambda) \exp\Big\{ \sum_{i=1}^{n} [-\sigma_i(\lambda) - \sigma_i'(\lambda) - \varepsilon_{\mathrm{R}}(\lambda) - \varepsilon_{\mathrm{M}}(\lambda)] N_i L \Big\} + B(\lambda) \quad (1)$$

where, $I(\lambda)$ and $I_0(\lambda)$ are the light intensities with and without absorption by the trace gas at the wavelength λ and optical path L. The cross section $\sigma_i(\lambda)$ and $\sigma_i'(\lambda)$ represent the narrow spectral structures and the broad spectral features, respectively. The Rayleigh extinction and Mie extinction of aerosols are described by $\varepsilon_{\mathrm{R}}(\lambda)$ and $\varepsilon_{\mathrm{M}}(\lambda)$. N_i denotes the concentration of trace gas and the noise $B(\lambda)$. A polynomial of a specified degree is used to filter the broad variation. The remained narrow structure is defied as the optical density:

$$\ln \frac{I_0}{I} = \sum_{i=1}^{n} \sigma_i N_i L + B'(\lambda) \quad (2)$$

Concentration of NO_3 is retrieved using least-squares fits of NO_3 reference spectra to the optical density.

III. THE EFFECT OF WATER VAPOR ON NO_3

The analysis of the nitrate radical is carried out in the visible red spectral region from 640 nm to 680 nm to include the NO_3 radical absorption peak centered at 662 nm. Water vapor strong absorption is also found in this region. The influence of water vapor is critical for the NO_3 evaluation because overtone bands of the water vapor peak at 651.5 nm are very close to NO_3, which could affect the precision and detection limits of the DOAS system [23-27].

In the DOAS technique, reference cross sections must be subjected to a linear fit to the measured optical density. It is implicit that the reference cross section does not change shape with changing of column density. Under tropospheric conditions, water vapor mixing ratios usually vary from 0.01% to 5%, giving column densities from 1.36×10^{21} molecules/cm^2 to 6.8×10^{23} molecules/cm^2. At these high water vapor column densities, the linearity assumed by the Lambert-Beer law breaks down and saturation of some absorption lines is often achieved.

Figure 2 is the calculated absorption lines by HITRAN at the high resolution of 0.005 nm. Calculated optical densities of water vapor absorption using the low resolution of the spectrograph (0.48 nm) and maximum mixing ratios of 0.18, is shown in Fig.3. But the maximum value reached up to 0.18, while the maximum value of the measured optical density based on DOAS is below 0.09 (see Fig.4). What appears at low resolution to be a fairly weak absorption (Fig.4) is actually com-

DOI:10.1088/1674-0068/21/05/433-437

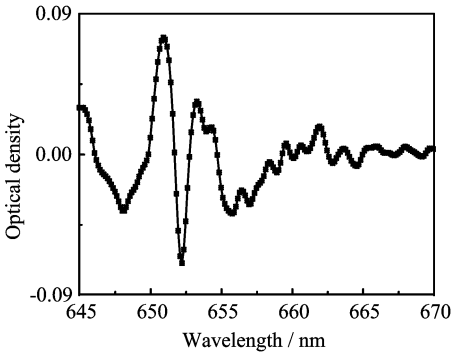

FIG. 4 Measured optical densities at the low resolution.

posed of a number of very strong absorption lines seen at high resolution (Fig.2). The nonlinearity of water vapor absorption is obvious in the DOAS measurement. Therefore, the convoluted cross section of water vapor is not used to retrieve the absorption of water vapor.

But nitrate radical only exists at detectable concentrations during the nighttime. The daytime atmospheric absorption spectra (at solar zenith angles <80°) can serve as reference spectra for eliminating water vapor absorption, but the column density of water vapor varies between daytime and nighttime.

Although the overall cross section is not a linear function of column density of water vapor, the cross section of water vapor was found to be a different linear function at each wavelength over the range of column density of water vapor [21]. The cross section at a particular relative humidity is therefore related to that at another relative humidity for constant pressure by the following expression:

$$\sigma_{\mathrm{OD}} = \sigma_{\mathrm{OD}_0} + \frac{\mathrm{d}\sigma_{\mathrm{OD}}}{\mathrm{d}RH}\Delta RH \tag{3}$$

here, σ_{OD_0} is the reference cross section of water vapor based on the daytime atmospheric absorption spectra at a chosen column density of water vapor, σ_{OD} is the reference cross section at another column density, and ΔRH is the difference between the two relative humidities. It is possible to adjust the reference cross section to be at the correct column density in the fitting process. $\mathrm{d}\sigma_{\mathrm{OD}}/\mathrm{d}RH$, derived from the smoothed reference cross sections of the daytime atmospheric absorption spectra, describes the difference between the cross section used. Therefore, an achieved reference cross section that would better describe the water vapor absorption, is essentially a fit to minimize the residual.

Reference spectra of water vapor were calculated based on the daytime atmospheric absorption spectra, and the change of cross section with relative humidity ($\mathrm{d}\sigma_{\mathrm{OD}}/\mathrm{d}RH$) for a particular column amount was fitted simultaneously with the cross section for that particular column of water vapor. This process gave a more accurate fitting of water vapor absorptions.

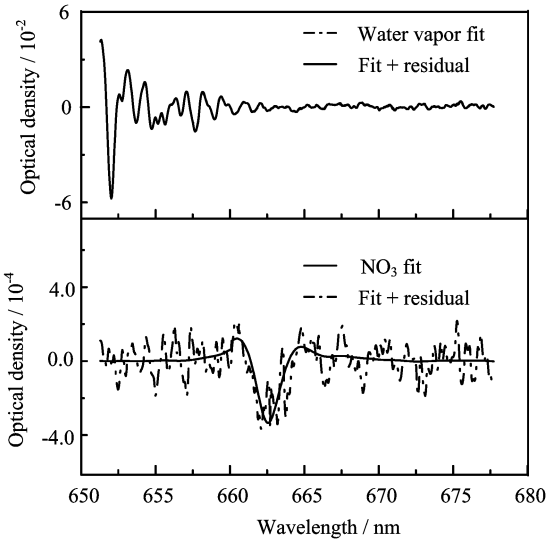

FIG. 5 The effect of the interpolated reference spectrum at close studied night.

IV. SPECTRA ANALYSIS OF NO_3

The absorption feature centered at 662 nm from 650 nm to 680 nm was used for quantification of NO_3 concentration [28-35]. The cross section σ(662 nm)= 2.25×10^{-17} cm^2 (http://www.atmosphere.mpg.de/) was used for the NO_3 evaluation. Apart from the NO_3 radical, the main absorber was water vapor in that region. The water vapor reference section was achieved based on the aforementioned processing technique, and was fitted simultaneously with the reference cross section of nitrate radical.

Stay light, electronic offset, and dark current were corrected from the measured atmospheric spectra. The logarithm of the resulting spectrum was then numerically high pass filtered and the result was then low pass filtered, resulting in the measured optical density. The reference spectra of NO_3 and the water vapor were fitted to the measured optical density simultaneously based on a least squares routine after they were subjected to the same filtering technique.

The reference spectrum, which was obtained by interpolating daytime spectra to achieved water reference spectra at the various relative humidity, was chosen to fit the water vapor absorption at the same relative humidity, resulting in the best results (see Fig.5). It was found that the effect of water vapor absorption was restricted to a minimum. The detection limit was 3.6 ppt according to residual. If only the daytime spectra which were close to the studied night were interpolated to get a water vapor absorbing spectrum, the detection limit was 4.6 ppt according to residual.

This approach was found to be most successful in removing the water vapor absorption since it offered the flexibility to account for variations in column densities of water vapor. The effect of water vapor absorption

DOI:10.1088/1674-0068/21/05/433-437

was restricted to a minimum.

The Pearl River Delta is one of the areas which have experienced the fastest economic development in China. In consequence, coal smog and traffic exhaust together cause serious photochemical smog and particulate pollution problems on a large scale both in urban and regional areas. In order to understand the role of NO_3 in the nighttime, NO_3 was measured by LP-DOAS, from June 30 to July 10, 2006 in the back garden are (23°28′86″N; 113°02′91″E) of Guangzhou during an intensive field campaign in the Pearl River Delta.

LP-DOAS setup was deployed on the third floor and an array of retro-reflectors was placed in another building resulting in a total atmospheric optical path of 3.1 km on the average, 10 m above the ground. There was a lake under the optical path and many trees and grasses around the measurement site. The integration time of the measurement spectra was adjusted automatically to the incoming light intensity, so the nitrate radical could be retrieved every 2-15 min by evaluating the spectral range between 640 and 680 nm. Figure 6 was the time series of the concentrations of NO_3, which were subjected to the aforementioned processing technique. Its nighttime average was 23.6±1.8 ppt with the detection limits 3.6 ppt. NO_3 at these levels can play a significant role in oxidation of VOCs [1,31].

The levels were slightly higher than those shown in several previous studies that also used LP-DOAS. But the significantly higher mixing ratios were often found in polluted air masses by Brown *et al.* using a cavity ring-down spectroscopy (CaRDS) instrument for *in situ* quantification of both NO_3 and N_2O_5 [7,16].

V. CONCLUSION

The real-time and in-line measurement of trace-gas concentration can be performed by LP-DOAS technique, which is widely applied to study and monitor the quality of the environment. For the nitrate radical, LP-DOAS is an appropriate technique. But the strong absorption of water vapor affects the precise measurement of nitrate radical and the detection limits of the LP-DOAS system. Reference cross section, when used together with change of cross section with water vapor column densities, was found to give better fits for the purposes of accurate nitrate radical analysis. Using this technique, the detection limits of the LP-DOAS system for nitrate radical reached 3.6 ppt. The modified method was applied during an intensive field campaign in the Pearl River Delta, China. The average level of NO_3 was 23.6±1.8 ppt in polluted air masses.

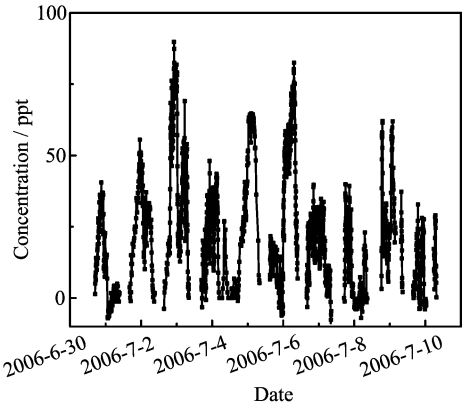

FIG. 6 Time series of the concentrations of NO_3.

VI. ACKNOWLEDGMENTS

This work was supported by the National High Technology Research and Development Program of China (No.2007AA12Z109) and the Natural Science Foundation of Anhui Province University (No.KJ2008A114). We acknowledge DOAS groups and Peking University for their help.

[1] A. Geyer, B. Alicke, S. Konrad, T. Schmitz, J. Stutz, and U. Platt, J. Geophys. Res. **106**, 8013 (2001).
[2] S. S. Brown, Geophys. Res. Lett. **33**, LO8801 (2006).
[3] M. Winer, R. Atkinson, and J. N. Pitts, Science **224**, 156 (1984).
[4] B. J. Allan, N. Carslaw, H. Coe, R. A. Burgess, and J. M. C. Plane, J. Atmos. Chem. **33**, 129 (1999).
[5] M. O. Andreae and H. Raemdonck, Science **221**, 744 (1983).
[6] S. W. Li, W. Q. Liu, P. H. Xie, A. Li, M. Qin, F. M. Peng, and Y. W. Zhu, J. Environ. Sci. **20**, 45 (2008).
[7] S. S. Brown, H. Stark, T. B. Ryerson, E. J. Williams, D. K. Nicks Jr., M. Trainer, F. C. Fehsenfeld, and A. R. Ravishankara, J. Geophys. Res. **108**, 4299 (2003).
[8] C. E. Edward, J. Zhao, and R. Zhang, Anal. Chem. **76**, 5436 (2004).
[9] J. Stutz, B. Alicke, R. Ackermann, A. Geyer, A. White, and E. Williams, J. Geophys. Res. **109**, D12306 (2004).
[10] A. Geyer, B. Alicke, D. Mihelcic, J. Stutz, and U. Platt, J. Geophys. Res. **104**, 26097 (1999).
[11] U. Platt, D. Perner, G. W. Harris, A. M. Winer, and J. N. Pitts, Geophys. Res. Lett. **7**, 89 (1980).
[12] S. W. Li, W. Q. Liu, P. H. Xie, A. Li, and M. Qin, Adv. Atmos. Sci. **24**, 875 (2007).
[13] S. R. Aliwell and R. L. Jones, J. Geoph. Res. **103**, 5719 (1998).
[14] U. F. Platt, A. M. Winer, H. W. Blermann, R. Atkinson, and J. N. Pltts Jr., Environ. Sci. Technol. **18**, 365 (1984).
[15] J. Stutz and U. Platt, Appl. Opt. **35**, 6041 (1996).
[16] S. S. Brown, T. B. Ryerson, A. G. Wollny, C. A. Brock, R. Peltier, A. P. Sullivan, R. J. Weber, W. P. Dubé, M. Trainer, J. F. Meagher, F. C. Fehsenfeld, and A. R. Ravishankara, Science **311**, 5757 (2006).
[17] D. Mihelcic, D. Klemp, P. Msgen, H. W. Pätz, and A. Volz-Thomas, J. Atmos. Chem. **16**, 313 (1993).

DOI:10.1088/1674-0068/21/05/433-437

[18] F. Heintz, H. Flentje, and R. Dubois, J. Geophys. Res. **101**, 22891 (1996).
[19] N. Carslaw, L. Carpenter, J. Plane, B. Allan, R. Burgess, K. Clemitshaw, H. Coe, and S. Penkett, J. Geophys. Res. **102**, 18917 (1997).
[20] J. Stutz, B. Alicke, R. Ackermann, A. White, and E. Williams, J. Geophys. Res. **109**, D12306 (2004).
[21] S. R. Aliwell and R. L. Jones, Geophys. Res. Lett. **23**, 2585 (1996).
[22] R. P. Wayne, I. Barnes, P. Biggs, J. P. Burrows, C. E. Canosa, G. Restelli, and H. Sidebottom, Atmos. Environ. **25**, 1 (1991).
[23] A. Geyer, *The Role of the Nitrate Radical in the Boundary Layer*, Ph. D. Dissertation, Institute of Environmental Physics, University of Heidelberg, (2000).
[24] J. P. Burrows, G. S. Tyndall, and G. K. Moortgat, J. Phys. Chem. **59**, 4848 (1985).
[25] A. R. Ravishankara and P. H. Wine, Chem. Phys. Lett. **101**, 73 (1983).
[26] U. Platt, *Differential Optical Absorption Spectroscopy, in Monitoring by Spectroscopic Techniques*, M. W. Sigrist, Ed., New York: John Wiley, (1994).
[27] A. Geyer and U. Platt, J. Geophys. Res. **107**, D204431 (2002).
[28] S. S. Brown, J. E. Dibb, H. Stark, M. Aldener, M. Vozella, S. Whitlow, E. J. Williams, B. M. Lerner, R. Jakoubek, A. M. Middlebrook, J. A. DeGouw, C. Warneke, P. D. Goldan, W. C. Kuster, W. M. Angevine, D. T. Sueper, P. K. Quinn, T. S. Bates, J. F. Meagher, F. C. Fehsenfeld, and A. R. Ravishankara, Geophys. Res. Lett. **31**, L07108 (2004).
[29] C. A. Stroud, J. M. Roberts, E. J. Williams, D. Hereid, W. M. Angevine, F. C. Fehsenfeld, A. Wisthaler, A. Hansel, M. Martinez-Harder, H. Harder, W. H. Brune, G. Hoenninger, J. Stutz, and A. B. White, J. Geophys. Res. **107**, 4291 (2002).
[30] M. Vrekoussis, M. Kanakidou, N. Mihalopoulos, P. J. Crutzen, J. Lelieveld, D. Perner, H. Berresheim, and E. Baboukas, Atmos. Chem. Phys. Disscuss **3**, S2003 (2003).
[31] N. Smith, J. M. C. Plane, C. F. Nien, and P. A. Solomon, Atmos. Environ. 29, 2887 (1995).
[32] E. C. Wood, T. H. Bertram, P. J. Wooldbrige, and R. C. Cohen, Atmos. Chem. Phys. **5**, 483 (2005).
[33] M. Vrekoussis, M. Kanakidou, N. Mihalopoulos, P. J. Crutzen, J. Lelieveld, D. Perner, H. Berresheim, and E. Baboukas, Atmos. Chem. Phys. **4**, 169 (2004).
[34] R. P. Wayne, I. Barnes, P. Biggs, J. P. Burrows, C. E. Canosa-Mas, J. Hjorth, G. LeBras, G. K. Moortgat, D. Perner, G. Poulet, and H. Sidebottom, Atmos. Environ. **25**, 1 (11991).
[35] L. K. Amekudzi, B. M. Sinnhuber, N. V. Sheode, J. Meyer, A. Rozanov, L. N. Lamsal, H. Bovensmann, and J. P. Burrows, J. Geophys. Res. **110**, D20304 (2005).

DOI:10.1088/1674-0068/21/05/433-437